LUND UNIVERSITY

FACULTY OF SCIENCE - PHYSICS

DIVISION OF SYNCHROTRON RADIATION RESEARCH

InAs and High-k Oxides

A Scanning Tunnelling Study of their Interfaces

Author:
Mattias ÅSTRAND

Supervisor:
Dr. Rainer TIMM
Co-supervisor:
Andrea TROIAN

Thesis submitted for the degree of Bachelor of Science

Project duration: 2 months

Spring 2018

LUNDS UNIVERSITET

Contents

Abstract ii

Acronyms and Abbreviations iii

1 Introduction 1
- 1.1 Band Structure . . . 2
- 1.2 Reciprocal Space and Miller Indices . . . 4
- 1.3 Scanning Tunnelling Microscopy and Spectroscopy . . . 4
- 1.4 Degassing, Annealing and Atomic Layer Deposition . . . 6

2 Experiment 7
- 2.1 Setup . . . 7
- 2.2 Procedure . . . 8
  - 2.2.1 Sample Preparation . . . 8
  - 2.2.2 Sample Cleaning . . . 8
  - 2.2.3 STM Tip Preparation . . . 9
  - 2.2.4 Sample Microscopy . . . 9
  - 2.2.5 Sample Spectroscopy . . . 10
  - 2.2.6 Comparing Spectra from Clean and High-k Covered Surfaces . . . 10

3 Results and Discussion 12
- 3.1 Surface Characterization and Measurement Reproducibility . . . 12
  - 3.1.1 InAs(111)B . . . 14
  - 3.1.2 InAs(100) . . . 17
- 3.2 Band Structure Analysis . . . 18
- 3.3 Interface States . . . 21

4 Conclusion and Outlook 22

Acknowledgements 24

Abstract

In order for semiconductor materials to be suitable for implementation in new and progressive devices they have to be of better electronic characteristics than currently used materials, and maintain these once treated and put into action. It is important to verify that bulk characteristics are not hindered at the surface when a given semiconductor is put in contact with another material due to necessity. In particular, one may want to isolate the surface of a semiconductor from the ambient, and implement artificially grown insulators, such as some types of oxides, to do just this. It is then crucial to verify that the semiconductor's value is not compromised by it being put into contact with the insulator.

III-V semiconductors are very promising, in terms of electronic characteristics, when it comes to application in progressive devices. However, they are known to have defect-rich native oxides, which means that a number of different surface treatment techniques are required to replace them with better ones and ultimately allow for III-V implementation. Moreover, one has to make sure that interface quality between III-V semiconductors and artificially grown oxides is appropriate.

In this project, InAs (one of many III-V semiconductors) surfaces are considered, alongside the interfaces between them and thin HfO_2 (hafnium oxide, a highly insulating material) layers. Sample preparation is realised through annealing (under atomic hydrogen flow) for surface cleaning, and atomic layer deposition (ALD) for controlled deposition of insulating oxide. The main tools at hand for sample analysis consist in scanning tunnelling microscopes, hence the use of scanning tunnelling microscopy (STM) and scanning tunnelling spectroscopy (STS) to record data. All in all, it is deduced that electron states altering the standard InAs band structure are at times present at the interface between semiconductor and oxide, hinting at creation of imperfect samples. Nevertheless, the work carried out in this project should open the door for further investigation on what materials and laboratory procedures work best and will eventually meet optimal interface conditions.

Acronyms and Abbreviations

IC Integrated circuit

III-V Alloy of elements from the third and fifth group of the periodic table

STM Scanning tunnelling microscopy

STS Scanning tunnelling spectroscopy

VB Valence band

VBM Valence band maximum

CB Conduction band

CBM Conduction band minimum

BG Band gap

TIBB Tip-induced band bending

ALD Atomic layer deposition

UHV Ultra-high vacuum

XPS X-ray photoelectron spectroscopy

LDOS Local density of states

1 Introduction

Semiconductors are versatile materials that are found at the base of most, if not all, of our technological equipment. Thanks to their hybrid-like conducting properties, which classify them neither as conductors nor insulators, they are perfect for applications in which altering between conducting and non-conducting states is required.

For reasons that will soon become obvious, it is not surprising to find out that the development of devices such as transistors deeply relies on the proficiency of the semiconductor industry. Transistors are none other than microscopic components that form part of all Integrated Circuits (ICs) and are fundamental to processing units of all kinds. Semiconductors are at the core of transistor engineering and their electronic properties are exploited in such a way that ultimately results in a switch-like behaviour of transistors themselves. These operate by transitioning between an "on" and an "off" state, which correspond to there being current and no current flow, respectively. The current is carried via a semiconductor channel from one end (source) of the devices to the other (drain), and its flow is activated thanks to the application of a bias through the so-called gate. The latter is to be isolated from the semiconductor channel to prevent current loss. This is usually done by having an insulating layer, typically an oxide of high dielectric constant k, separating the two components. Note that dielectric is a synonym of insulator, hence k is a measure of how good an insulator a given material is.

Knowing the above, two fundamental conditions for the production of technologically advanced devices arise: the availability of semiconductor channels of great electronic properties, which goes hand in hand with the efficiency with which one can switch between conducting states, and the presence of good insulating materials to prevent signal loss. So far silicon has been the star of semiconductors in device construction, one of the main reasons for this being that its natural oxide SiO_2 (i.e. oxide which is naturally grown on the material as it gets in contact with air) is both a good insulator and basically free of defects that deteriorate current flow through the semiconductor channel. The same cannot be said for many if not all other semiconductor contenders, as their natural oxides tend to compromise their electronic properties at the surface level. Even though some semiconductors, such as multiple III-Vs (alloys of elements from the third and fifth group of the periodic table), have been shown to have better electronic properties than silicon [1], their application is not as frequent as one would expect. This is because choosing any of them would imply going through the tedious side-process of cleaning their surfaces from any native oxides and replacing them with desired high-k oxides. Sticking to silicon instead means that once a desired structure is grown in the laboratory, it can be directly implemented in device construction. Nevertheless, this material limitation will sooner or later have to be confronted and resolved if technological advance is desired to proceed at the same pace that has been maintained over the last decades.

At this point enough insight into the matter has been given to state the purpose of this project. This is none other than the exploration of the characteristics of InAs (indium arsenide, one of the mentioned III-Vs) surfaces. In particular, surfaces that have been cleaned are compared to those on which a thin layer of high-k oxide, HfO_2 (hafnium oxide), has been deposited. This is done in order to retrieve data about possible future applications in the semiconductor industry, and at the same time find optimal parameters for the operation of needed equipment and evaluate required techniques for surface treatment. The state of the studied surfaces is assessed by means of scanning tunnelling microscopy (STM), and their electronic properties inspected via scanning tunnelling spec-

troscopy (STS).

The reasons behind choosing InAs over any other III-V semiconductor are mainly its promising electronic properties. The material is known to have extraordinary electron mobility, thus offering the possibility for application in high frequency devices, along with a small band gap, meaning that small voltages would be enough to bias and operate InAs based technologies [2]. Moreover, some research has already been carried out on InAs at the division of synchrotron radiation in Lund, and further studies are welcome in order to achieve a more complete evaluation of the material.

In order to carry out and understand the studies in this project, a firm solid state background is required. Topics that are relevant to surface science are of particular interest. First of all, one needs to grasp those concepts that are related to band structure characterization of a given material. These are in fact crucial to the interpretation of gathered results. Secondly, the notions of real and reciprocal space must be understood. Miller indices, which correspond to a convenient notation for surface classification, indeed build upon the notion of reciprocal space, and are the tool used to distinguish between surfaces in this project. Since classification is not as central as a topic as surface characterization to this work, only the essential aspects of it will be hereby provided. Thirdly, the theoretical arguments in favour of the correct functioning of the adopted experimental procedures need to be introduced. As already given away by the name of the techniques themselves (STM and STS), the quantum mechanical effect of tunnelling is essential to the recording of data. The latter must therefore be explained to an adequate extent. Finally, a brief survey on the mechanisms that rule on the used surface treatment techniques will be given.

1.1 Band Structure

Similarly to how electrons surrounding the nucleus of an atom fill available levels of increasing energy, electrons in a solid occupy energy bands from lowest to highest energy. As opposed to levels, bands are continua of energy, and arise from having a large system of coupled (bound) atoms. To understand this statement a somewhat simplified example is presented [3]. Think of an Na (sodium) atom, which has one valence electron (outermost electron which takes part in the formation of bonds with other elements). Then consider an Na_2 molecule. In the formation of the latter, each of the involved Na atoms shares a valence electron to form what is known as a covalent bond. In this process, the atomic orbitals hosting the valence electrons of the two Na atoms overlap to give rise to a collective molecular orbital. It turns out that there are two possible outcomes of this overlap. The first being the creation of a bonding orbital of lower energy than the atomic orbitals (hence favouring the bonding of the elements into a molecule), the other being the formation of an anti-bonding orbital of higher energy. It goes without saying that the bonding orbital is naturally selected by the overlapping phenomenon. Now consider the case in which there are N Na atoms participating in a bond. Analogously, N states will be created, half of them being bonding states. The latter are fully occupied by the valence electrons following Pauli's exclusion principle (each state is occupied by two electrons of opposite spin, so to not have two or more fermions in the same quantum state). The greater N becomes, the closer in energy the resulting N states become. In the upper limit ($N \gg 1$) a quasi-continuum of states, call this energy band, is reached and is half filled by the Na valence electrons.

Now that the concept of energy band has been introduced, one can proceed with

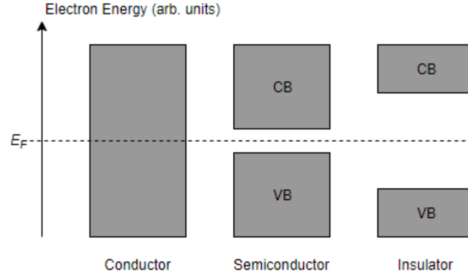

Figure 1: Material classification according to band gap size.

the classification of solids based upon different band structures. First of all, define the outermost occupied band as valence band (VB), the first unoccupied band as conduction band (CB), and the discrepancy in energy between the valence band maximum (VBM) and conduction band minimum (CBM) as band gap (BG). Secondly, define the quantity "Fermi level", or E_F, as the the energy level at which there is 50% probability of electron occupation. Note that this definition makes sense if one thinks of the transition between occupied to unoccupied states as smooth, and wants to know where filled electron states come to an end. Finally, let those materials that have a partially filled band around E_F be called conductors, while those that have completely filled VBs (E_F in BG) be called insulators. It might at first sight be strange to observe E_F inside the BG for insulating materials. However, the ambiguity ends when one simply thinks of the statistical nature of the quantity: E_F is found between the 100% probability of occupation of the VB and 0% occupation of the CB. A final class of materials, crucial to this project, arises if one makes a distinction between insulators with large and small BG. Typically, it is agreed upon that anything below 3 eV is small, and materials with such BGs are labelled as semiconductors.

Due to a phenomenon called doping, which essentially corresponds to the introduction of specific external agents into a semiconductor material, the Fermi level of the overall system can be shifted. This occurs thanks to the dopant having an abundance or scarcity of electrons. When electrons are abundant (n-doping), "donor" states are found close to the CBM and electrons from these can easily (at little energy expense) excite into the CB, effectively moving E_F towards the CBM. In the other case (p-doping), "acceptor" states appear close to the VBM and electrons from the VB can excite into them, shifting E_F towards the edge of the valence band. These two cases correspond to the possibility for creation of charge carriers in semiconductors: electrons in n-doping, and holes ("missing electrons") in p-doping. Essentially, the electronic properties of a semiconductor can be tweaked according to necessity via provision of adequate dopants.

By effects that are similar to the ones described above, other sorts of contaminations might influence the characteristics of semiconductors in an unwanted way. This is the case for native oxides and other contaminants that gather on to III-V's treated in this project [4]. Surface defects that arise from the oxidation of III-Vs give rise to an abundance of energy levels inside the BG. This effectively "pins" E_F at certain values and results in the semiconductor losing its susceptibility to charge carrier modulation when an external energy source acts upon it. In a transistor, this would result in the gate not being able to influence correctly the semiconductor channel, hence the device being compromised. The contaminants must be removed to restore the innate quality of studied surfaces.

1.2 Reciprocal Space and Miller Indices

When describing matter at the solid state, it is not a coincidence if a recurring pattern is found in the building blocks of a material. In fact, it holds that the disposition of atoms in crystals is at times periodic in such a way that it can be described as an array of points via a translational, three-dimensional vector of the type:

$$\mathbf{R} = n_1\mathbf{a_1} + n_2\mathbf{a_2} + n_3\mathbf{a_3} \tag{1}$$

Where $\mathbf{a_i}$, $i = 1, 2, 3$ are vectors in the (real) three-dimensions, and n_i , $i = 1, 2, 3$ are integers. A crystal system that can be described with equation 1 is referred to as a Bravais Lattice. Having stated this, one proceeds with the next relevant definition, the one of reciprocal lattice. This is nothing more than a Bravais lattice depicted in an auxiliary space (reciprocal space) where lattice periodicity follows the vector:

$$\mathbf{G} = m_1\mathbf{a_1^*} + m_2\mathbf{a_2^*} + m_3\mathbf{a_3^*} \tag{2}$$

m_i , $i = 1, 2, 3$ being integers and $\mathbf{a_i^*}$, $i = 1, 2, 3$ vectors in reciprocal space, related to $\mathbf{a_i}$, $i = 1, 2, 3$ in real space via $\mathbf{a_i} \cdot \mathbf{a_j^*} = 2\pi\delta_{ij}$.

The notion of reciprocal space might at first seem obscure, but its use becomes self explanatory when Miller indices are introduced. Imagine to cut the real lattice with a plane such that three points of the lattice are included in it. Proceed then with taking the inverse of the coordinates of such points in the space spanned by the $\mathbf{a_i}$ vectors, and multiply each of the inverses by a common integer so to obtain a new set of integers $(h\,k\,l)$. These are labelled as Miller indices and are used to describe sets of planes perpendicular to the direction $h\mathbf{a}_1^* + k\mathbf{a}_2^* + l\mathbf{a}_3^*$.

With the above at hand, saying that this project focuses on the study of InAs(100) and (111) surfaces should raise no further questions. To be even more specific, InAs(111)B is used, where the B indicates As surface termination.

1.3 Scanning Tunnelling Microscopy and Spectroscopy

What enables the studies in this project is the possibility to evaluate the state of a semiconductor's surface and understand the condition of its band structure. This can be done by implementing a scanning tunnelling microscope, a tool which owes its functioning to quantum tunnelling. To get a basic understanding of this, the case of an electron of energy E travelling in one dimension (x-direction) and meeting a potential barrier of thickness s and energy V_0 is considered. The electron can be described by the time-independent Schrödinger equation:

$$\left[\frac{-\hbar^2}{2m}\frac{\partial^2}{\partial x^2} + V(x)\right]\psi(x) = E\psi(x) \tag{3}$$

m being its mass, $V(x) = V_0$ inside the barrier and $V(x) = 0$ elsewhere. By introducing the variable $\kappa = \sqrt{2m(V - E)/\hbar^2}$, equation 3 becomes:

$$\psi''(x) - \kappa^2\psi(x) = 0 \tag{4}$$

Where $''$ indicates second derivative in x. Equation 4 is solved by wave functions of the form:

$$\psi(x) = \psi_0\, e^{-\kappa x} \tag{5}$$

ψ_0 being a constant. Due to the nature of κ (imaginary outside and real inside the barrier) the solution is an oscillation outside the barrier and an exponential decay inside the barrier. This translates to the possibility for the electron to "tunnel" through the barrier and propagate further with probability amplitude dampened by the exponential decay inside the barrier. It can then be shown that the probability for transmission of the electron through the barrier is given by $T = e^{-2\kappa s}$ [5].

Drawing analogies with the microscopy technique, a stream of electrons of energy E is provided thanks to the application of a bias $V_{bias} = E/e$ (e being the fundamental charge) between the tip of the microscope and the to-be-analysed surface. Furthermore, the separation of tip and sample acts as a potential barrier. It is then intuitive to conclude that the resulting tunnelling current I_t registered by the apparatus is proportional to T and thus depends exponentially on the tip-sample separation s and $E = eV_{bias}$ (as the latter is included in κ).

The actual case of tunnelling in the STM technique is technically and theoretically more involved (three dimensionality, wave function overlap of tip and surface atoms etc.). However, the insight given by the one dimensional case brings to the correct tunnelling current behaviour and is more than adequate for the level of this project.

It now comes to understanding how tunnelling is exploited in STM and STS. In the former technique the current arising due to electron tunnelling between tip of a microscope and surface atoms of a to-be-studied material is used to construct a reproduction of the surface itself. It is important to distinguish between two main methods for carrying out microscopy. These correspond to constant tunnelling current or constant vertical tip position. The former is the commonly adopted procedure, none other than the one used in this project. It corresponds to setting I_t to a fixed value, and allowing the vertical tip position to change throughout the scan. This automatically readjusts so to (in principle) always have the same tip-sample separation (as this maintains I_t constant). Its recording can be used to create a three dimensional surface profile of the scanned surface.

In order to have atomic level accuracy in regulation of the tip position, piezoelectric crystals are used. These are materials that generate more or less stress (and hence contract or dilate) if a given voltage is applied onto them thanks to the phenomenon of piezoelectricity [3]. What allows for the crystals to reshape and thus change the tip's position is a voltage feedback loop which constantly updates according to the displacement from the to-be-scanned surface. This drops an increasing or decreasing amount of voltage across the crystals depending on whether the tip is too close or too far from the sample, respectively.

Regarding STS, the status of the band structure of a studied material can be asserted by fixing the position of the tip above its surface and initiating a bias voltage sweep. At $V_{bias} = 0$, the tip's Fermi level coincides (energy wise) with the material's Fermi level E_F. As soon as V_{bias} is modified, one can picture the situation as the Fermi level of the tip being shifted from E_F by an amount eV_{bias}. Given a bias of large enough magnitude, the tip's Fermi level ($E_F + eV_{bias}$) will lie above the CBM or below the VBM of the sample, meaning that electron tunnelling from the tip to the sample's CB or from the sample's VB to the tip may be registered, respectively. More specifically, for a bias that is negative and of large magnitude the VB is met, whilst for large positive bias the CB is found. VB and CB present filled and empty states, respectively. Therefore, when scanning the VB, current will be registered from sample to tip (negative current in the produced spectra), and vice versa for the CB (positive current). For intermediate values of V_{bias}, no tunnelling will be registered due to the tip's Fermi level being in the BG of the studied material.

A reconstruction of the band structure of the studied sample emerges, as VB, BG and CB can be identified. One can then estimate the size of the band gap of the material by distinguishing the voltages at which tunnelling currents start to arise.

One final consideration to make is tip-induced band bending (TIBB). This is none other than the consequence of some of the applied bias voltage between the tip and the studied sample dropping in the sample itself. When a non-zero V_{bias} is applied, the electric field which is established between the tip and the sample ultimately brings to the bending of bands. Amongst the parameters which play a role in determining the magnitude of TIBB one finds the distance between the tip and the sample and the tip's radius [6]. This effect is a constant obstacle to accurate spectroscopic results, as the band bending might impede tunnelling just above the CBM and below the VBM of the studied sample (influencing the estimate of the size of its BG), and needs to be accounted for.

1.4 Degassing, Annealing and Atomic Layer Deposition

When it comes to the treatment of surfaces, three distinct techniques are of interest to this project. Specifically, degassing and annealing, which focus on the removal of surface contaminations and unwanted native oxides, and atomic layer deposition (ALD), which aims at depositing a thin slab of desired high-k dielectric onto a given surface.

Degassing is the process of heating up a sample up to the point at which particulates that are found at the surface of the sample become loose and eventually detach. The reason for this happening can be attributed to surface adhesion being of lower strength than the forces keeping a bulk of constituents together. It is common knowledge that surface particulates are less tightly bound than bulk ones due to them not being surrounded by as many other atoms (to whom they may bond) as they would be in the bulk.

Annealing consists in a more intense heat treatment than degassing, and has the purpose of fundamentally changing a sample at its surface level. In this project, steady sample heating is combined with atomic hydrogen flow to clean surfaces from unwanted species (native oxides in particular). Hydrogen radicals, being highly interactive, are very likely to bond with contaminants at the surface level. Volatile products thus arise and are easily removed from the sample's proximities.

In STM and STS it is of vital importance to work in a clean environment. One needs to make sure that what is being scanned is the sample and the sample only. It is thus common practice to implement degassing to remove any unwanted contaminants on sample holders, then proceed with annealing to eliminate contaminants on sample surfaces.

ALD is a technique which allows for the deposition of thin films of highly controlled thickness (at an atomic level). It is carried out thanks to the provision of chemicals which react with a sample surface in a complementary fashion [7]. One generally has two gaseous reactants, referred to as precursors, to whom the to-be-covered surface is exposed to. Each of these is provided in an adequate abundance and prepares the surface to exposure to the other reactant by saturating it with a monomolecular reactant layer [8]. What emerges from this is an overall self-contained, cyclic process. Each step of the film growth continues until the reactant that is being used has finished interacting with the surface by laying out exactly a single layer. This is the characteristic which allows for a high level of process control.

2 Experiment

The assessment of surface and interface properties of InAs surfaces (with and without high-k oxides) in this project is realised by means of analysis in an STM setup. The composition of such a system will be discussed, alongside the necessary equipment and procedures which are necessary for the creation and inspection of InAs samples.

2.1 Setup

Throughout the course of this project, a total of two scanning tunnelling microscopes was available, both similar in construction except for one of them operating at room temperature, and the other being equipped with a cryostat, hence presenting the possibility to operate at approximately 10 K thanks to liquid helium cooling. The former was used in InAs(100) measurements. The latter was implemented in InAs(111)B measurements, and the available cooling should have been enough to eliminate unwanted temperature dependent effects (such as vibrations, thermal broadening and drift). Figure 2 portrays an example of scanning tunnelling microscope, which reproduces the features of the mentioned systems closely.

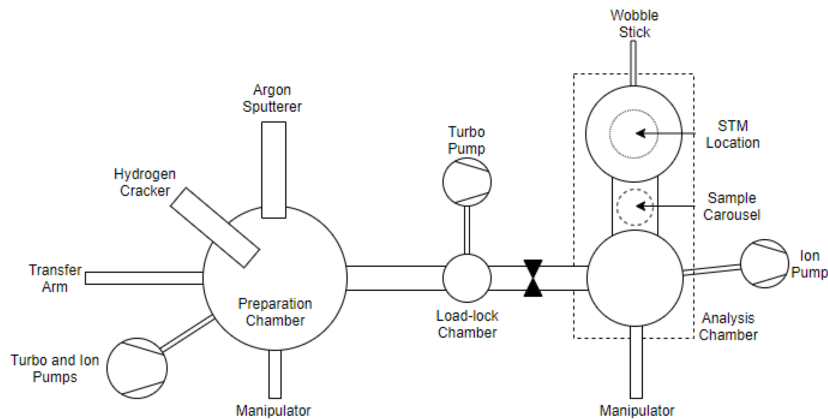

Figure 2: Schematic showing a scanning tunnelling microscope setup comprehensive of the characteristics of those used in this project.

An STM setup is typically made up of two main airtight chambers, the preparation and the analysis chamber. These are connected to each other by a pipe with a valve which can be used to isolate them from one another. Each of them is equipped with vacuum pumps that aim at reducing pressure in the system until the ultra-high vacuum (UHV) regime is reached (10^{-9} mbar and below). The reason for operation of the system at UHV is simple: samples that are prepared and brought into the system are then cleaned of those impurities that they naturally gather in a standard atmospheric pressure environment (e.g. the laboratory). One then wants to keep the sample immaculate whilst it is being studied, something that would not be possible if the microscope setup was not being pumped to maintain low pressure, as the sample would once again start to collect impurities. The pumping is also crucial to stabilising pressure after in situ procedures that involve streams of particles being released into the system. A load-lock chamber is present and used to insert samples into the system. Transfer arms, manipulators and wobble sticks are the mechanical arms used to move samples in the system once it is sealed. Furthermore, many samples can be stored in the system at the same time thanks to a

carousel, typically placed next to the actual microscope location in the analysis chamber. The preparation chamber, as hinted at by its name, is where samples are brought when first introduced into the system and necessary pre-microscopy treatments are applied. The chamber is equipped with a hydrogen cracker (for annealing under atomic hydrogen flow) and an argon sputtering source (for removal of impurities that gather on metallic objects, such as new tips for the device). Moreover, thanks to a power supply connected to the manipulator in the preparation chamber, temperatures can be raised on demand via resistive heating on samples held by the manipulator itself (required both for degassing and annealing).

The above presented information about STM chambers applies well to the systems implemented in this project.

2.2 Procedure

2.2.1 Sample Preparation

The preparation of InAs samples studied in this project can be divided into a number of different steps. First of all, a few fragments of a surface area of about 5×5 mm^2 are cut out of thin InAs(100) and InAs(111)B wafers stored in sealed containers. This is done using a diamond-tip pen, with which carving out shapes along specific directions of the crystals is easy. Half of the gathered samples is then brought to the ALD facility where ALD of HfO_2 is carried out. The latter is done using tetrakis (dimethylamino) hafnium (TDMAH) and water as precursors (preheated at 75 °C), proceeding with cycles at 120 °C until layers of just over 1 nm have been formed [9]. Note that no cleaning is required prior to ALD since the latter is known to yield "interface self-cleaning". That is, the deposition of high-k material automatically results in a reduction of native oxides at the interface between oxide and coated sample [7]. In the meanwhile, sample holders compatible with the transferring mechanisms in the sealed microscope chambers are degassed at around 200 °C while laying on the manipulator of a preparation chamber. Finally, complete samples are assembled by heating the holders on a simple heating surface (up to $\sim$ 190 °C), melting metallic indium on them and using it as a glue to hold InAs fragments. The created samples host a substrate fragment and a fragment undergone ALD of hafnium oxide, both of them having either the (100) or the (111)B surface. This way, the comparison between clean surface and interface between substrate and high-k oxide is facilitated for surfaces of the same type, as the two sample types can be analysed subsequently and efficiently if present on the same holder.

2.2.2 Sample Cleaning

Samples prepared according to the above procedure are brought into one of the two available microscopes, specifically in its preparation chamber. Here, they are gradually heated up to 380-390 °C via resistive heating applied thanks to the power supply linked to the manipulator in the chamber. Degassing of weakly bonded contaminants occurs as the samples get warm, and unwanted native oxides are removed with further treatment. As the final temperatures are approached (at 300 °C and above), the hydrogen cracker in the chamber (a tungsten filament) is carefully brought to incandescence ($\sim$ 1700 °C) in order to be able to "crack" hydrogen molecules (H_2) into hydrogen radicals (H^*). Hydrogen flow is initiated by leaking hydrogen directly in the cracker unit, thereby altering the pressure in the whole chamber due to sudden input of atomic hydrogen. The leaking is adjusted

so to obtain a pressure of $2 \cdot 10^{-6}$ mbar in the chamber. Once this condition is matched, the "shutter" (a plate found just below the cracker) is removed so to allow direct flow of H^* onto a to-be-cleaned sample. The system is then left under these circumstances for 30 to 45 minutes, and this is what one refers to as annealing under atomic hydrogen flow [10].

Once the time for annealing has elapsed, the procedure is shut down by first terminating the hydrogen leak, then gradually lowering the temperature of the filament and of the sample in this order. If one were to cool down the sample first, it could happen that hydrogen still present in the chamber gathers at the sample surface, overall yielding a H-terminated surface. It might also be that the filament desorbs some impurities via degassing while still warm, and deposits these on the sample itself. If the sample is the last one to be cooled down, it is also the last one to degas and thus has lower chance to collect impurities.

2.2.3 STM Tip Preparation

An object that is of vital importance to STM is the scanning tip. A few words shall thus be spent on their preparation.

A section of W (tungsten) wire of 0.8 mm diameter and arbitrary length (a few cm) is cut and then brought a few mm deep in a NaOH (sodium hydroxide) etching solution (electrolyte). Electrochemical etching [11] is carried out until the submerged part of the wire gets cut off and what remains is a tip sharp at the atomic level. The reason for the cutting to be this sharp lies in the the way in which etching is carried out. The to-be-cut wire acts as the anode of the etching system, as it is connected to the positive pole of a direct current loop. The cathode of the loop (linked to the negative current pole) is a secondary tungsten filament submerged in the NaOH. As the etching procedure is carried out, particulates are dissolved where the anode meets the electrolyte (NaOH solution) and are at the same time deposited on the cathode. The solution surrounds the wire, thus carves from outside inwards. Eventually, in the atomic regime, the link between the submerged part and the dry part of the anode becomes too weak to hold the two together and breaks, ultimately forming a sharp tip. The etched wire is brought out of the etching station and cut adequately to fit a tip holder (of roughly 0.4 cm^3 in volume), into which it is permanently fixed via clamping with a pair of pliers. To further sharpen the tip and clean it off impurities at the surface level, it is sputtered with Ar (argon) in the preparation chamber of an STM system. The sputtering process consists of creating a direct flux of Ar ions onto the tip, with a strength such that the pressure in the chamber reaches the value of $2 \cdot 10^{-5}$ mbar, and maintaining it for half an hour. The tip is handled in the chamber thanks to a magnetic holder, which allows for the removal of old tips and placing of new ones in the analysis chamber once the sputtering process is terminated.

2.2.4 Sample Microscopy

Samples that have undergone adequate cleaning procedures are ready to be imaged in the analysis chamber. Once they have been brought here and placed in the dedicated slot above the STM tip, the tip itself can be approached and scanning can be initiated.

There are two steps in the tip approach: the first one being manual approach until a safe distance to the naked eye (aided by an optical camera) is reached, the second being automatic approach. That is, the tip is allowed to make continuous (atomic) steps towards the surface, whilst at all steps letting the piezoelectric crystals go from fully contracted to

fully extended. The approach is complete once a pre-set tunnelling current I_t is registered by the equipment, with the crystals being in a relaxed position (neither too contracted nor dilated).

Adequate parameters to use in the approach are a sensitive feedback loop, a tunnelling current of $I_t \approx 50$ pA, and bias of $|V_{bias}| \approx 2.5V$. It is to be noted that it is not necessary to keep these the same during microscopy. Too high sensitivity might result in the tip readjusting too violently whilst scanning, hence compromising resolution. Furthermore, one may consider increasing I_t to 100 pA, as higher current corresponds to shorter tip-sample separation, hence potentially better resolution. As long as the chosen V_{bias} corresponds to either the VB or the CB of the scanned sample, it is not necessary to change it, as tunnelling would only be compromised by scanning in the BG. One could safely drop to bias magnitudes of 1-1.5 V, knowing that the BG of InAs is small (well below 1 eV [2]).

Once the approach is complete scanning in constant current mode can be initiated.

2.2.5 Sample Spectroscopy

At any point during a scan, one may fix the position of the tip above the studied surface and carry out spectroscopy. When doing this, V_{bias} is allowed to gradually shift from a pre-set lower limit to an upper one, perhaps from -1 to 1 V, and resulting changes in I_t are recorded. It is common practice to scan over a small area surrounding the chosen spectroscopy location to ensure good surface conditions and that measurements are not being taken on, for example, surface defects. Furthermore, one might be interested to further highlight the exact voltages at which the bands and the BG meet. To do this, one allows the tip to move closer to the sample (typically by 1 Å per V [12, 13]) as the absolute value of V_{bias} approaches 0. By doing this, I_t values are magnified until V_{bias} reaches values corresponding to the BG, where I_t is 0 in any case. The latter is known as Feenstra mode, and is implemented in some STS results in this project.

2.2.6 Comparing Spectra from Clean and High-k Covered Surfaces

In the following, it is going to be explained how the above mentioned procedures are put together in order to collect data in the laboratory.

One starts by considering either an InAs (100) or (111)B sample, comprehensive of a substrate fragment and another that has undergone ALD of HfO_2. If the sample is newly made, it is introduced into the system and put through a first round of annealing under atomic hydrogen flow. If carried out with the correct set of parameters (as described in section 2.2.2), the cleaning procedure should not affect the deposited high-k oxide, as recent X-ray photoelectron spectroscopy (XPS) measurements have shown [14]. Therefore, after the annealing procedure, one should have a clean InAs surface on one fragment and a clean interface between substrate and HfO_2 layer in the other.

As previously mentioned, comparison between clean surface and clean interface measurements is the focus of the carried out experimental work. When it comes to the analysis of samples, a few complications arise when organising work in order to yield rigorous comparison. The greatest concern is to avoid drastic changes to the probe (tip) of the microscope between scans. In case of deformation or collection of contaminations by the latter, scanning conditions change and likely deteriorate, making comparison between different results difficult if not worthless. The adopted procedure thus makes sure that as little changes as possible are caused to the tip when changing from plain surface to

the same type of surface, yet covered by a thin layer of HfO_2. The procedure itself is explained in the following.

After bringing the sample in the analysis chamber, the clean surface part is approached first. Scanning is initiated to verify that the cleaning procedure was effective (lumps of oxide and other substantial surface contaminations, spread throughout the whole surface, would indicate unsuccessful cleaning). If need be, a second annealing procedure is carried out. Else-wise STM is continued until a satisfyingly flat region is found. Here STS is carried out in different locations, looking for reproducibility in the measurements. This would highlight good surface stability and not just luck-related results. Once satisfied with the amount of gathered data, the tip is retracted and then approached to the surface presenting the thin insulating slab. Here STM is not initiated as there is little interest in scanning over an oxide layer. This would result in nothing more than an image of the covered surface, blurred by the need to tunnel through the oxide itself (note that tunnelling through the latter is only possible due to it being thin). Instead, the tip is left to stabilize after the approach to avoid experiencing drift (acting too impetuously would result in distorted measurements as the piezoelectric crystals need time to find equilibrium). Spectroscopy measurements are then taken. If not convincing, only then microscopy is started to help decide upon a different region for STS. It is easy for the tip to adsorb or desorb materials whilst scanning, especially on the sample with HfO_2, since the oxide layer dampens tunnelling and the tip might approach too much (and perhaps even crash) to maintain a high pre-set current value. Therefore, it is of interest to move the tip as little as possible after relocating it from the clean surface to the oxide covered one, as this would mean that measurements are being taken with essentially the same tip conditions.

If at some point the tip seems to not respond, yield unreliable adjustments in height (of several Å and perhaps even nm instead of in the order of magnitude of atomic steps) and randomized spectroscopic measurements, it most likely got deformed. This is taken care of with either a tip conditioning or a controlled tip crash into a gold surface. The former implies a high voltage pulse ($\sim$ 7 V) applied on the tip with the purpose of removing impurities and sharpening it. The latter is a way to coat the tip with a highly conductive metal to make it once more a reliable probe for microscopy and spectroscopy. As long as the tip works fine, microscopy and spectroscopy are continued, all in all going back and forth between substrate and ALD samples until a satisfying amount of data has been gathered.

3 Results and Discussion

Measurements taken throughout the course of this project are presented below, accompanied by some discussion regarding their validity, meaning and implications. Examples of micrographs (STM results) are given for surfaces before and after their annealing under H flow, so to appreciate the efficiency of the cleaning technique. Spectra (STS results) for the cleaned surfaces and those put through ALD of HfO_2 are presented, both for the InAs(100) and (111)B samples. Furthermore, an idea of band structure evolution throughout the surfaces will be given thanks to spectroscopic measurements taken at different locations (for example flat areas, terraces, atomic steps, lumps etc.). From this it should emerge whether results are consistent over space and time, or if the samples are contaminated even after their treatment. The characteristics setting apart cleaned and ALD samples of the same InAs surface, and the ones differentiating InAs(100) from InAs(111)B are also described.

3.1 Surface Characterization and Measurement Reproducibility

To start things off, an image of an unclean surface is presented, followed by an example of an annealed surface. To best appreciate the details in these micrographs, a three-dimensional version of them is presented, created with the aid of the program Gwyddion [15].

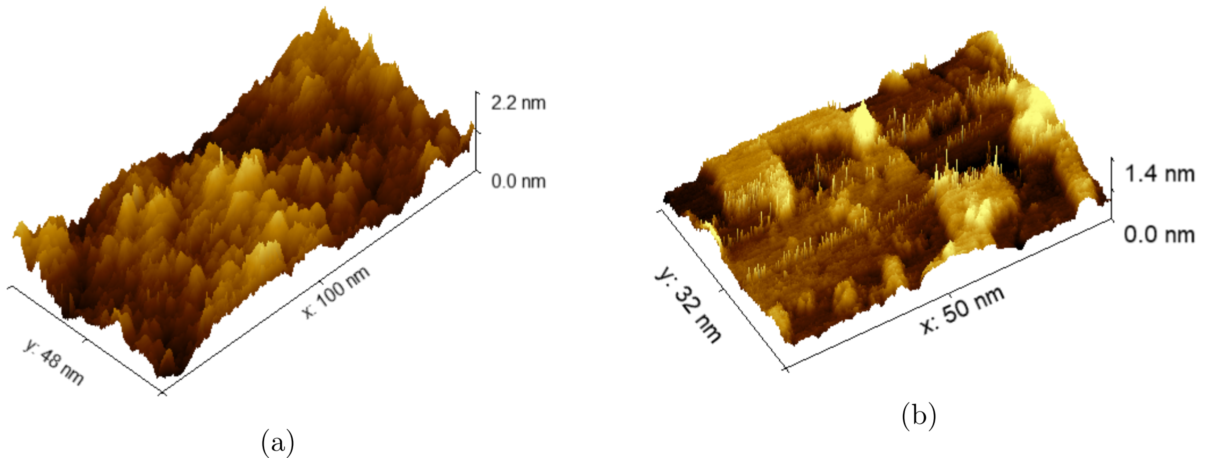

(a) (b)

Figure 3: STM of an unclean (a) and clean (b) InAs(100) surface. (a) was taken with -1.5 V bias and 150 pA preset current, whilst (b) with -1.5 V bias and 100 pA preset current.

As it can be seen, the differences between the two are quite evident. Figure 3a presents an uncountable number of lumps and irregularities throughout the surface, whilst Figure 3b portrays ample flat regions bounded by atomic steps. Evidently, accumulated native oxides and surface contaminations of other sorts made it so that the tip had to readjust often in height while recording Figure 3a, whilst the successfulness of the annealing procedure removed most of the mentioned oxides and allowed for steady imaging in Figure 3b. Some lumps are still present in the latter, probably caused by contaminations of other sorts than native oxides (which could not be removed through annealing, or accumulated after the cleaning procedure), however they are of much less weight towards the determination of the smoothness of the scan.

It is to be noted that this surface comparison, of before and after successful annealing, is analogous for the InAs(111)B sample. Even though InAs(100) and InAs(111)B are different at the surface level, their response to the cleaning procedure is similar in the sense that starting from plentiful accumulated oxides one arrives at smooth (mainly oxide free) surfaces. Clean InAs(100) and InAs(111)B surfaces will be further treated in the following.

As previously mentioned, annealing under H^* flow also takes care of native oxides at the interface between InAs surfaces and high-k layers. However, this aspect is not evaluated by means of comparison of "before and after" micrographs, mainly because of the already mentioned obstacles that arise when scanning over an oxide layer. A micrograph (see Figure 4) taken over a sample covered by HfO_2 is nonetheless provided with the intent of highlighting difficulties that arise when scanning over an oxide.

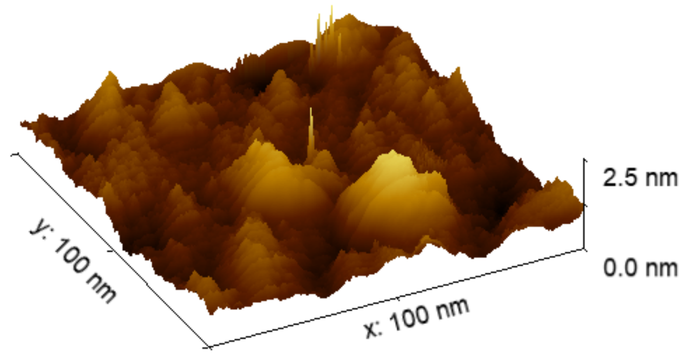

Figure 4: Micrograph of an InAs(111)B surface covered by HfO_2, taken with -2 V bias and 100 pA preset current.

The possibility to detect signal when scanning over samples coated by insulating material is a consequence of the insulating layer itself being thin enough for the microscope to register tunnelling through it. This same reason allows for the probe to not crash during an approach, and readjust throughout a scan. STM over an oxide is nonetheless a delicate matter. The signal recorded by the microscope is dampened no matter how thin it is, thus complications arise when trying to record meaningful scans over surfaces that have undergone the ALD procedure. It would to some extent make sense to compare Figures 3a and 4. Even though ALD is a much more precise deposition technique than natural oxidation (hence the fewer lumps in Figure 4), it nonetheless ends up covering the studied surface with an oxide slab, and similarities between the figures cannot be dismissed. Films created by the ALD conditions used here are very thin, yet amorphous and thus not presenting flat terraces on the surface. Overall, resulting micrographs appear as being disordered, thus one can draw the conclusion that it is less worth it to perform microscopy and more worth it to collect spectra over those samples that present thin HfO_2 layers.

Now that the matter of microscopically clean surfaces and interfaces has been introduced, characterization of these by means of spectroscopy is the natural next step. It seems reasonable to state that the band structure of a semiconductor material as a whole is of a given shape, characterized by specific E_F, VBM and CBM positions. However, it is also reasonable to assume that these bulk characteristics might not be attained at the surface, where rearrangement of atoms and bonding with both wanted (e.g. high-k) and unwanted (e.g. native oxides) contaminants may alter the appearance of the band structure. It is then quite intuitive to conclude that different treatment is required for the

(100) and (111)B surfaces as they present different terminations, surface reconstructions and potentially different behaviour when subjected to ALD and other experimental techniques. This topic is at the core of the following paragraphs, where the reproducibility of spectroscopy throughout different surfaces is evaluated in order to understand whether the surfaces are consistent with themselves or measurements are highly dependent on when and where they are taken. The latter would highlight questionable material choice or unreliable performance of the available laboratory equipment.

3.1.1 InAs(111)B

Firstly, as seen in Figure 5, the case for a clean InAs(111)B surface is treated. Specifically, an image recorded over such a surface is presented along with some numbered locations at which spectra were taken. It is to be noted that Figure 5a was recorded in the cryostat-equipped microscope, operating at a temperature of about 10 K. Furthermore, spectra shown in Figure 5b were all recorded in Feenstra mode. This means that displayed currents are artificially increased towards small applied bias. As previously mentioned, this should emphasize the onset of the VB and the CB for each spectrum.

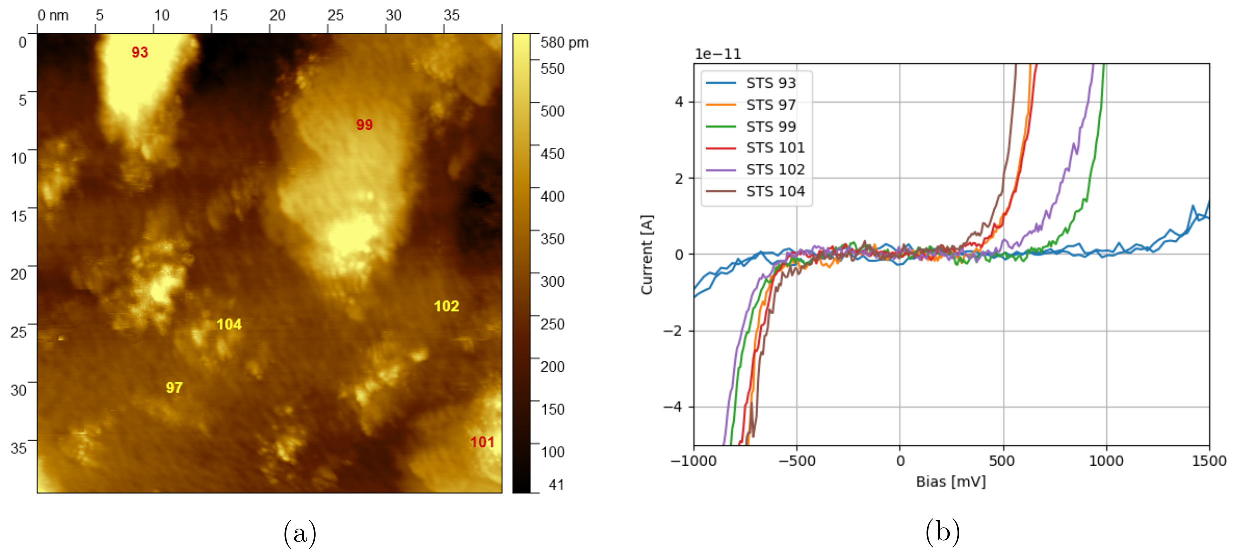

(a) (b)

Figure 5: Micrograph (-1.5V bias, 180 pA preset current) of a clean InAs(111)B surface on which multiple (marked) spectra have been taken (a). Spectra corresponding to the labels on the scan (b).

The characteristics of the studied InAs(111)B patch are captured in Figure 5a. It can be seen how a few lumps (possibly corresponding to remaining impurities) are still present, scattered throughout the micrograph. The major one being the accumulation in the top left of the micrograph. At the same time, it can be appreciated how the overall shape of the scanned area is otherwise smooth, even presenting a well defined terrace (flat region displaced upwards by an atomic step with respect to its surroundings) in the top right.

A few more words shall be spent on a phenomenon that seems to have affected the micrograph precisely around this terrace. It can be noted how the latter does not drop immediately to a lower atomic level to the left, but instead takes two steps down. This is an artefact arising from a condition known as "double tip", where the tip of the STM is forked and presents two sharp ends instead of a single one. What follows is contemporary

scan by both ends, hence reappearance of features already outlined by the first tip as the second one scans over them again.

Moving on to spectroscopy, one can easily distinguish the typical characteristics of a semiconductor's band structure in the curves in Figure 5b. In fact, all of these undoubtedly present a VB, a BG and a CB. Whether these features match for different results is another story.

One spectrum in particular, the one numbered 93, stands out for being quite inconsistent with the others, especially regarding the CB onset. It is to be noted that it coincides with the analysis of the tallest point in the scan, which is most likely not a coincidence. It is quite likely that the lump on which spectrum 93 was taken consisted with a contamination of insulating properties, presenting a BG larger than the one of InAs. This would help to explain the BG in spectrum 93 being over half an eV larger when compared to the other measurements. Regarding the other spectra, they agree much better with each other, especially about the onset of the VB (which seems to occur at around -0.5 V). In the positive voltage region, spectrum 99 seems to meet the CBM later than the other curves. Even though the offset is not as large as for spectrum 93, it is still not satisfyingly close to the other spectra to safely state that results are perfectly reproducible throughout the whole surface. A promising aspect about the results is that they all portray a band gap of reasonable size. However, the latter always appears as larger than the literature value for InAs at low temperatures, 0.43 eV at 0 K [16]. It might be so that the expected 0.43 eV BG is actually the case in curves such as 97, 101 and 104 in Figure 5b, however the resolution of the spectra themselves is not high enough to draw a trustworthy conclusion. In fact, noise in the zero-current region makes it quite hard to state accurate estimates of VB and CB onsets. Another explanation for the BG being larger than expected might be found in TIBB.

Moving on to results gathered on the InAs(111)B sample coated in HfO_2, a collection of spectra is shown in Figure 6. These were also taken in the low temperature microscope. Furthermore, the reason for there to be more than one curve of the same colour is that multiple voltage sweeps were carried out at the same location once a spectroscopic measurement was commenced.

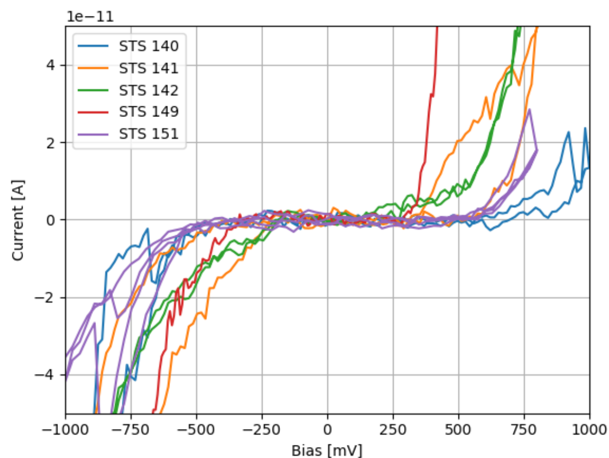

Figure 6: Selection of spectra carried out on an InAs(111)B surface covered by a high-k layer.

An important result, which stands out in Figure 6, is that clear current signals arise

far below ± 1 V. This indicates that tunnelling through the HfO_2 layer is efficient enough to completely mask the oxide's band structure and directly show the features of InAs. In fact, the BG of HfO_2 lies between 5.3 and 5.7 eV [17], and greatly exceeds the relevant bias range in Figure 6.

It is pleasing to see that, except for spectrum 141, sweeps performed at the same position are quite consistent with each other (curves of the same colour seem to trace out the same features over and over). However, the variety of results appears to take different stances on what band structure characterizes the HfO_2 coated sample. Spectra 140, 149, 151 and even 141 seem to point out that the sample is not compromised in the sense that it behaves like a semiconductor. Not only that but spectra 140 and 151 even seem to take the same position on BG size as most of the results displayed in Figure 5b. STS 149 suggests a smaller BG (which is expected for InAs), and 141 agrees with it for one of its sweeps, whilst it agrees with 140 and 151 for the other sweep. This inconsistency might be a consequence of tip instability during the spectroscopy that yielded result 141. Regarding STS 142, instead, the behaviour highlighted by the sweeps is clearly metallic. This is understood from the fact that no matter what bias is applied, there is always a resulting tunnelling current. The consistency between sweeps in STS 142 also points at this not being a coincidence but an actual property of the analysed spot on the sample.

There are a number of possible explanations for this, and it is somewhat hard to discern which one of them is the correct one. In particular, it could be that the tip desorbed some particulates whilst scanning over the surface, and that one of these was aimed at while taking STS 142. Another explanation is the presence of contaminations in the interface between substrate and HfO_2 layer, which yield electron states where one should merely observe the InAs BG. As previously mentioned, the InAs(111) samples used in this project are of type B, i.e. presenting As surface termination, and As itself is known to bond with other As atoms and form dimers. These end up imposing electronic states inside the natural InAs BG, yielding tunnelling where there would usually be none. Of course As dimers are not enough to explain "total" metallic behaviour, as they merely add states at a specific BG position and could not account for current at all biases. However, they might play a role in the overall behaviour, especially if in combination with contaminations (that cannot be eliminated via the annealing procedure). In hindsight, it seems reasonable to state that the argument raised in favour of As dimer creation should not only hold at all spectroscopy locations (hence affecting all the curves in Figure 6), but also for the mere clean surface. It is difficult to state whether this is actually the case. Nonetheless, it can safely be said that additional states (due to defects of some sort) are present at the interface between InAs(111)B and HfO_2, with variations locally on the sample (justifying sparse reproducibility). One last potential explanation is the "glue" that was used to hold the sample on the holder. As previously mentioned, this is none other than In (indium), and careless application of samples onto their holders could potentially have led to In-contaminations on the surface. This is the least likely cause of trouble, given the attention to detail that was put into sample creation, yet it is worth mentioning.

Taking into consideration other spectra, not here presented to avoid result overflow, it can be stated that the majority of results hint at little to no interface state contribution towards tunnelling currents at electron energies corresponding to the semiconductor's BG. That is, most results agree on the fact that a general semiconductor-like band structure is attained (with the unmistakable presence of a BG), and only a few exceptions depict the sample as being compromised by interface states which yield metal-like spectroscopy. What undermines reproducibility of results is the proposition of seemingly non-matching

BG sizes by different spectra, as already seen in Figure 6. BG size estimation is a delicate matter that goes hand in hand with the identification of VB and CB onsets, which might appear as different depending on the resolution and magnification of a plotted spectroscopy. That is why it will be further explored later in this section. Overall, it can be concluded that the range of characteristics displayed by the results in Figures 5 and 6 points at somewhat unpredictable reproducibility of spectroscopic measurements throughout the InAs(111)B sample, especially in the case of the high-k covered surface.

3.1.2 InAs(100)

The same kind of data treatment received by the InAs(111)B samples is extended to the (100) ones and presented in Figures 7 and 8. These samples were studied in the other available microscope (due to unavailability of the first during later stages of the project).

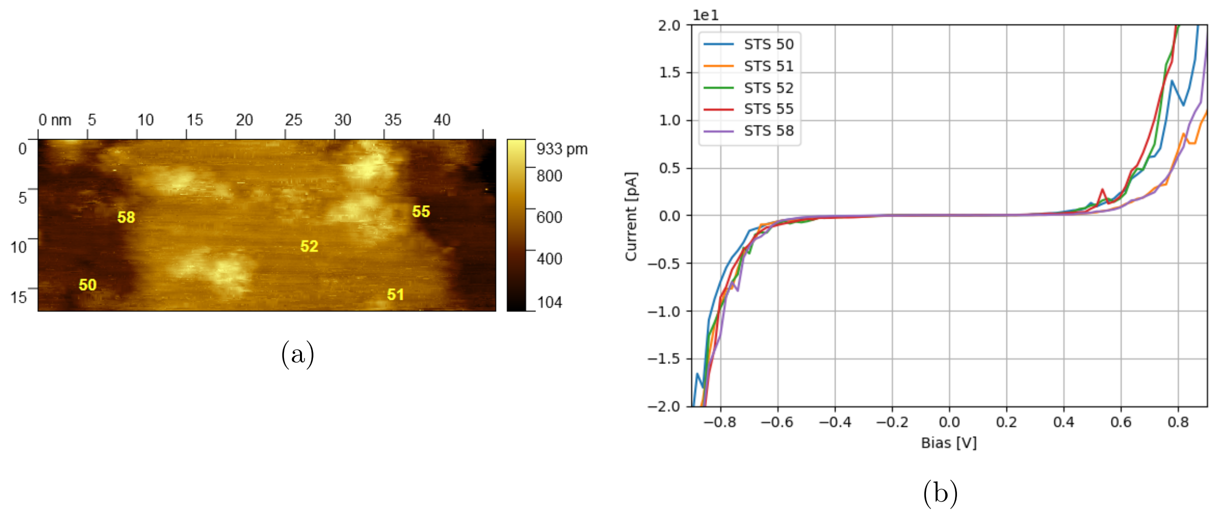

Figure 7: Micrograph (-2 V bias, 100 pA preset current) of a clean InAs(100) surface on which multiple (marked) spectra have been taken (a). Spectra corresponding to the labels on the scan (b).

Figure 7a shows a cleaned InAs(100) surface from which a number of different spectra were extracted. These are labelled and presented in Figure 7b. It is impressive to see how consistent these are, especially in the low bias region. Regarding what the spectra tell about the band structure, it is clear that a semiconductor-like behaviour is attained, yet it is difficult to take a definite stance on what BG size characterises it. According to literature, the BG of InAs at ambient temperature (300 K) is of 0.36 eV [16]. Looking at Figure 7b, this seems like a credible estimate for BG size, especially because the region between -0.2 eV and 0.2 eV seems to yield negligible magnitudes of tunnelling currents, while at neighbouring voltages the tunnelling current faintly rises. Overall, it can safely be stated that spectra are quite reproducible throughout the sample, and that they seem to reproduce the expected BG size.

Figure 8 depicts a number of spectra taken on an InAs(100)/HfO_2 sample. It is obvious that the reproducibility of results is at most mediocre. While there are some spectra (such as 129 and 130) that hint at unmistakable semiconductor-like band structure, others (127, 128) softly point at metallic behaviour of the surface (even if just faintly, they report tunnelling currents also at very small absolute voltages, meaning little to no BG).

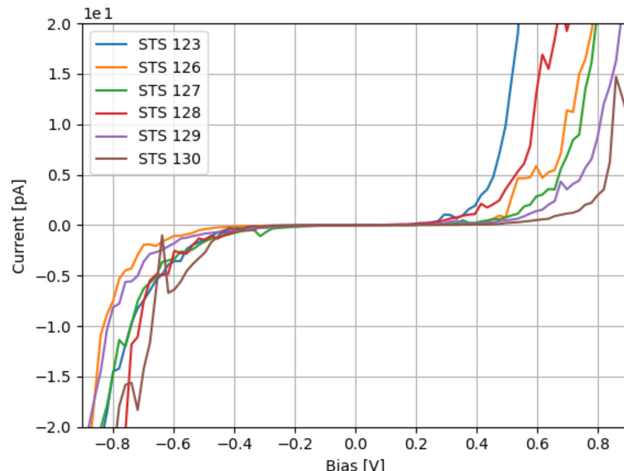

Figure 8: Selection of spectra taken across an InAs(100) surface covered by a HfO_2 layer.

The general conclusion to draw is that HfO_2 covered samples seem to present more electronic states than cleaned substrates, thus exhibiting tunnelling currents even at low absolute bias. This goes both for the InAs(100) and (111)B samples, though it applies more rigorously to the former. What also holds is poor reproducibility of spectroscopy, which makes the estimation of BG size an arduous task. Again, this seems to affect InAs(100)/HfO_2 more. Regarding the clean substrates, both the (100) and the (111)B surfaces present conventional band-structure features and better reproducibility. However, the BG of the (111)B surface seemed to be larger than expected from literature, an effect that could be attributed to TIBB.

3.2 Band Structure Analysis

To look deeper into the matter of band-structure characterization of the InAs samples, details of typical spectra (see Figure 9) are presented and discussed for each sample. In Figure 9, vertical dotted lines are used to indicate VBM, CBM and E_F positions, and horizontal dotted lines are used to indicate the point below which any current measurement is considered as noise. The choice of presented spectra aims at collecting characteristics consistently observed throughout the course of the project. Logarithmic (base 10) scale is used for currents in order to highlight the onsets of VB and CB.

Figures 9a and 9b show characteristic STS results for InAs(111)B with and without HfO_2 film, respectively. The reason for there to be more than one curve in the plots is that the data that was thought of as best representing the samples in their entirety was recorded over several sweeps (inter alia, of impressive reproducibility). Even though there are some current peaks reaching above the chosen noise threshold of 1 pA, these are considered to be mere fluctuations and are disregarded in the following. What then stands out is the similar band structure of the two InAs(111)B samples. Both characteristic spectra depict a VB onset near -0.55 V and CB onset at about 0.3 V, corresponding to a BG of approximately 0.85 eV. This is larger than the literature value of 0.43 eV, yet the difference might be attributed to TIBB. One could then speculate that InAs semiconductor behaviour is generally not compromised by the deposition of the high-k oxide HfO_2 on the (111)B surface. Another aspect that is worth mentioning is that E_F appears to be closer to the CB than to the VB, highlighting n-doping of the (111)B surface

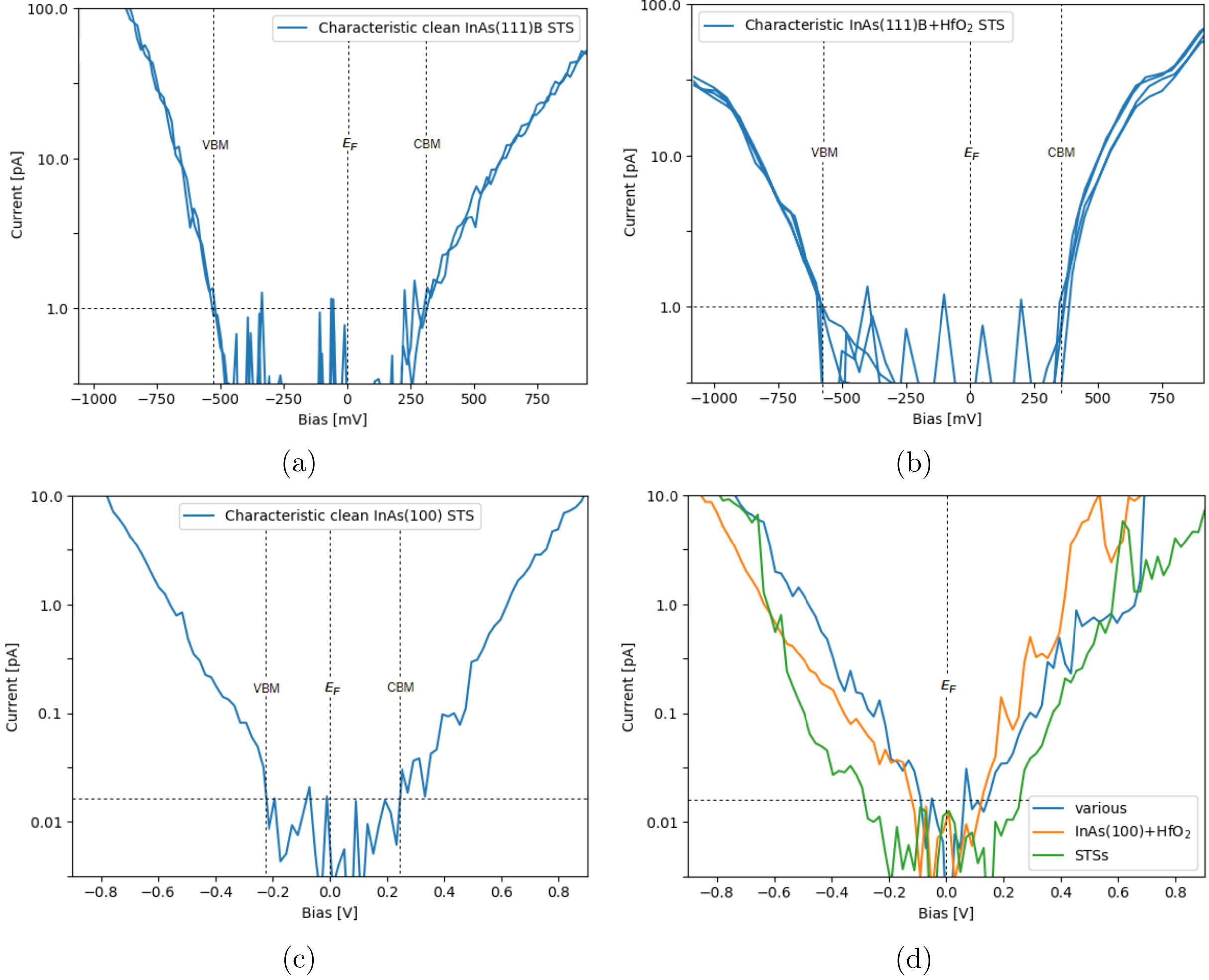

Figure 9: STS data plotted in semi-logarithmic fashion, showing typical band structure measurements for clean (a) and HfO_2 covered (b) InAs(111)B samples, and clean (c) and HfO_2 covered (d) InAs(100) samples.

(with and without insulating layer).

In section 3.1.1, where InAs(111)B samples were considered, it was concluded that spectroscopy is location dependent and of unreliable reproducibility for those surfaces that are coated in HfO_2. Even though this still is a valid statement, the magnification granted by logarithmic scale reduced the number of disagreements in BG size. In fact, it showed that many spectra actually agreed on VB and CB onsets, only linear scale could not provide high enough resolution to observe this. One should nonetheless be careful when jumping directly to the conclusion that the sample treatment carried out in this project was capable of creating an ideal interface between InAs(111)B substrate and HfO_2 layer. Regardless of the exceptions that show different behaviour than the one in Figure 9b, one can be satisfied about having a great number of measurements agreeing with it.

The same cannot be said for the InAs(100) samples. While the clean surface sample yielded spectra of expected (or at least consistent) shape, the HfO_2 coated sample displayed a vast variety of results, even when presented in semi-logarithmic fashion. Figure 9c, representing the clean InAs(100) surface, displays an average curve of two STS measurements that were considered to be equally capable of summarizing the general band structure of the sample. Due to current fluctuations at the edges of VB and CB, it was

difficult to decide upon exact VBM and CBM positions. Nonetheless, the chosen values of around -0.2 V and 0.25 V, respectively, yield an estimate of BG ($\sim$ 0.45 eV) that is not far from the (room temperature) literature value of 0.36 eV. Again, one could blame this offset on TIBB. Furthermore, the positioning of E_F is rather mid-gap, hinting at neither n- nor p-doping.

If estimating an appropriate value for clean InAs(100) substrate was not straight forward, discerning the shape of the band structure of the HfO_2 coated sample is an even harder task. As previously hinted at, this is a consequence of not having good result reproducibility. In fact, choosing a single STS to represent common sample features was not possible. Instead, three extremes are shown in Figure 9d. The blue curve shows almost metallic behaviour. The orange one has a more well defined BG, but with a size of only $\sim$0.2 eV. Finally, the green curve portrays a band structure similar to the one belonging to the clean InAs(100) surface, hence semiconductor-like and of a BG slightly larger than 0.4 eV. It seems safe to conclude that the interface between InAs(100) and deposited HfO_2 is far from perfect, presenting numerous electronic states at energies that would else-wise correspond to the BG of InAs, hence the recurring shrunk displacement between VBM and CBM, and even metallic behaviour.

It is interesting to notice that surface reconstruction (rearrangement of atoms at the surface level) on the clean InAs surfaces seems to not have affected spectra on neither of the InAs qualities. Reconstruction could potentially alter the appearance of a band structure by adding surface states at specific energy levels, yet this is not observed in Figures 9a and 9c, as no states are distinguishable in the BG of the clean samples.

Comparison between InAs(111)B results and those from InAs(100) ultimately reduces to consistent semiconductor-like behaviour for clean surfaces of both InAs qualities, and more consistency for InAs(111)B than for (100) when it comes to samples coated in HfO_2. Therefore, one may say that results that are gathered on InAs(111)B samples are more satisfactory than the ones derived on InAs(100). It is worth mentioning that two InAs(100) samples were actually created and studied to make sure that the fluctuations in the spectra were not a coincidence. This confirms the above drawn conclusion about InAs(100) and HfO_2 interfaces, and that the interface between HfO_2 and InAs(111)B surfaces is of better quality. This might, however, be a side-effect of using different machines for the measurements on the two InAs qualities. The microscope used for InAs(111)B (the one with the cryostat, which itself is a clear advantage) is new and equipped with more sophisticated or modern versions of the same tools that the other microscope possesses. Moreover, the microscope used for InAs(100) samples suffered from some defects in the preparation chamber throughout the course of the project. The leak valve used to allow hydrogen flow in the chamber broke, making the adjustment of correct pressure during annealing procedures challenging. Furthermore, the link between a dedicated power supply and the hydrogen cracker malfunctioned a couple of times, suddenly making voltage across the piece of equipment drop, along with its temperature. These two aspects combined could potentially have caused improper annealing of samples, or even their deterioration in the long term, making following treatments not fully effective. Finally, a power shortage once occurred, which turned off the vacuum pumps acting on the chamber. This could have caused contamination of the working environment and later of the samples, as they were being transferred between different areas of the machine.

3.3 Interface States

So far it has been mentioned that a variety of interface states might be present between InAs surfaces and HfO_2 layers, which could reshape the characteristic band structure of the semiconductor material as seen by an STM. It thus seems appropriate to conclude this section with further evidence gathered in favour of interface states.

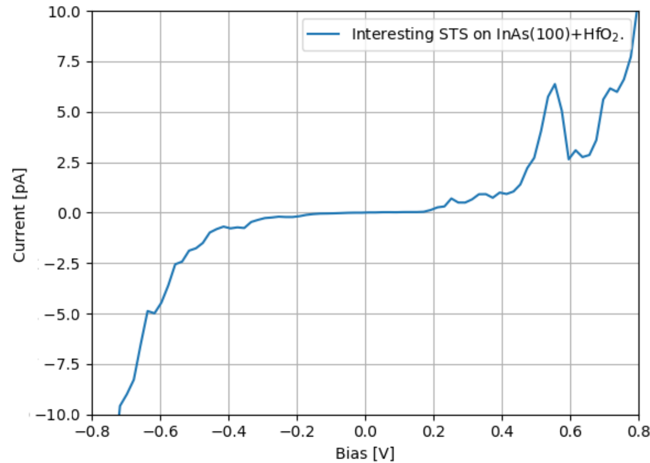

Figure 10: Spectrum taken on the InAs(100)/HfO_2 sample which presents a current peak at a bias of around 0.5 V.

Throughout the course of the project, when collecting STS data on InAs/HfO_2 samples, tunnelling current peaks appeared more than once at specific bias values, hinting at the localization of specific energy states at the interface between substrate and high-k oxide. Most of these peaks were not recurrent enough to be deemed as reliable (they might just as well have been coincidental noise). However, one peak in particular was observed regularly at ~ 0.5 V bias on the InAs(100)/HfO_2 sample, and is believed to point at some recurrent interface state created between the substrate and the high-k oxide. An example of spectrum which features this peak is shown in Figure 10.

Unfortunately, the tools that are adopted in this project are not enough to understand what the peak corresponds to. Microscopy can spot locations that seem to host contaminations, and spectroscopy can identify energies corresponding to given electron states (such as the peaks discussed so far). However, neither of them can discern the construction of a contamination, which might be a desirable feature to study. This leaves room for growth in future laboratory work and data analysis.

4 Conclusion and Outlook

Further consideration of the results gathered throughout the course of this project brings to a number of realisations regarding the adopted procedure and setup, how they might be improved, and possible future extensions to the carried out work.

To start things off, one may want to recall that the prominent purpose of this project was of characterising semiconductor and high-k oxide interfaces, in particular those between InAs surfaces and HfO_2. This was possible thanks to STS especially, and the artificially oxidized surfaces were compared with their clean counterparts to see the effect that deposition of HfO_2 had on the band structure of the semiconductor material (as experienced at the surface level). Ideally, one would have wanted to observe (consistently) little to no difference between clean and ALD samples. This would have highlighted little interference on the electronic properties of the semiconductor by the high-k, a result that is sought in the application of III-Vs in modern industry. However, suboptimal reproducibility of results was obtained, together with proof of band structure alteration due to the high-k, especially regarding the (100) surface.

The fact that results were gathered in different microscopes for the two studied surfaces makes them somewhat less comparable. Of course state of the art equipment and procedure should lead to equivalently reliable results. However the differences between the two used systems (e.g. the cryostat in one microscope and the unfortunate events in the other) might have had a role in ultimately determining the quality of results. The first comment that is going to be made on the laboratory procedure consists in the advise to try to measure the samples again, both on the same system, and (if time allows) on opposite systems to those that were dedicated to them in this project. In this way, results for InAs(100) and (111)B both at room and at liquid helium temperature would be collected. Furthermore, it is common practice to record the derivative of tunnelling current with respect to applied bias when taking STS data, and plot this (instead of crude tunnelling current) against bias itself. This is because $\frac{dI_t}{dV_{bias}}$ is directly related to the local density of states (LDOS) of the scanning point and thus leads to a more accurate band structure reconstruction [18]. To record this derivative, a lock-in amplifier is required, which was not implemented throughout the project. The second comment on the procedure thus consists in recommending the calibration of such an instrument to ultimately produce more valuable results.

In hindsight one could conclude that the combination of InAs and HfO_2 might be suboptimal. It is difficult to state for certain whether material incompatibility is the issue, or if further surface treatment would be required to create an ideal semiconductor-high-k interface. Nonetheless, it would be nice to proceed with the study of other III-Vs (for instance GaAs) or have HfO_2 exchanged for another valuable high-k material (e.g. Al_2O_3, that is, aluminium oxide). Moreover, one could extend the list of tools at hand to carry out the interface studies so to comprehend XPS or other tools capable of deducing the composition of surface particulates and eventual contaminants. As previously mentioned, the experimental techniques included in this project cannot recognise and understand contaminating materials and the sources of interface states. The addition of supplementary experimental techniques might shine light on what prevents from achieving ideal semiconductor-high-k interface and thus lead to the design of more efficient surface treatment routines.

All in all, it can be agreed upon that the work performed throughout this project shows the many obstacles that implementation of III-Vs in modern industry is facing. Further re-

search in the field is required to arrive at good and easily produced III-V surfaces, isolated from their surroundings or other pieces of equipment by non invasive (electronically-wise at the surface level) high-k layers. Nevertheless, the fact that some desirable result consistency was attained (especially for InAs(111)B) hints at a bright future for III-Vs. Not only would their implementation be revolutionary to the semiconductor industry, offering the possibility to work faster and at lower energy consumption than current technologies, but taking into account what has been learned in this project one can savour the achievement of always better interface conditions in the foreseeable future.

Acknowledgements

First and foremost, I would like to express my gratitude to Dr. Rainer Timm for making this thesis possible and guiding me through important stages of the project. I am honoured to have had the chance to work for Lund's synchrotron radiation research department and have had access to multiple technologically advanced facilities.

Special thanks to Andrea Troian for being available from the very beginning and providing priceless advice in the laboratory, for being an excellent mentor and a good friend. I am glad to have met someone that shares my interests in studies and free-time both, to whom I can even speak in my mother tongue.

Among other people that I have met in this journey, I would also like to thank Yen-Po Liu, for additional support in the laboratory and for being a dear friend.

Needless to say, I am grateful for being surrounded by people who care about me and always push me to do my best. A huge thank you to all of my friends, old and new alike. Thank you Maria, for being patient, encouraging and loving at all times. Your support is irreplaceable. Thank you Lucas, for being the best little brother in the world. Last but not least, thank you mom and dad, for helping me find my way in this world, making me the person that I am today and assisting me in the pursuit of all my dreams.

References

[1] del Alamo, J.A. *Nanometre-scale electronics with III-V compound semiconductors*. Nature, volume 479, number 7373, pages 317-23, 2011.

[2] Milnes, A. G., Polyakov, A. Y. *Indium arsenide: a semiconductor for high speed and electro-optical devices*. Materials Science and Engineering B, volume 18, issue 3, pages 237-259, 1993.

[3] Philip Hofmann. *Solid State Physics. An Introduction.* 2nd edition. Weinheim, Germany: Wiley-VCH; 2015.

[4] Houssa, M., Chagarov, E., Kummel, A. *Surface Defects and Passivation of Ge and III–V Interfaces*. MRS Bulletin, volume 34, issue 7, pages 504-513, 2011.

[5] Gunnar Ohlén. *Phenomena of the quantum world.* Lund, Sweden: Lund University; 2016.

[6] Dong, Y., Feenstra, R.M., Semtsiv, M.P., Masselink, W.T. *Influence of Tip-induced Band Bending on Tunneling Spectra of Semiconductor Surfaces*. Nanotechnology, volume 18, number 4, 2007.

[7] Gougousi, T. *Atomic layer deposition of high-k dielectrics on III-V semiconductor surfaces.* Progress in Crystal Growth and Characterization of Materials, volume 62, issue 4, pages 1-21, 2016.

[8] Ritala, M., Leskelä, M., *Atomic layer deposition.* Chapter 2. In: H.S. Nalwa. *Handbook of thin films.* Burlington: Academic Press; 2002.

[9] He, G., Chen, X. Sun, Z. *Interface engineering and chemistry of Hf-based high-k dielectrics on III–V substrates.* Surface Science Reports, volume 68, issue 1, pages 68-107, 2013.

[10] Knutsson, J.V. et al. *Atomic scale surface structure and morphology of InAs nanowire crystal superlattices: the effect of epitaxial overgrowth.* Appl. Mat. Interfaces, volume 7, issue 10, pages 5748–5755, 2015.

[11] Ibe, J.P. et al. *On the electrochemical etching of tips for scanning tunneling microscopy.* Journal of Vacuum Science & Technology A: Vacuum, Surfaces, and Films, volume 8, issue 4, pages 3570-3575, 1990.

[12] Mårtensson, P., Feenstra, R.M. *Geometric and electronic structure of antimony on the GaAs(110) surface studied by scanning tunnelling microscopy*. Physical Review B, volume 39, issue 11, pages 7744-7753, 1989.

[13] Feenstra, R.M. *Tunneling spectroscopy of the (100) surface of direct band-gap III-V semiconductors*. Physical Review B, volume 50, number 7, pages 4561-4570, 1994.

[14] Troian, A. To be published.

[15] Open source software *Gwyddion*, version 2.50, Czech Metrology Institution, 2018. Available at: `http://gwyddion.net/`

[16] Stephen T. Thornton, Andrew Rex. *Modern Physics For Scientists and Engineers*. 4th edition. Boston, MA, USA: Brooks/Cole, Cengage Learning; 2013.

[17] Bersch, E. et al. *Band offsets of ultrathin high-k oxide films with Si*. Physical Review B, volume 78, issue 8, number 085114, 2008.

[18] Wiesendanger, R. *Scanning Probe Microscopy and Spectroscopy: Methods and Applications*. Cambridge, UK: Cambridge University Press; 1994.